Molecular Crystals and Liquid Crystals

Publication details, including instructions for authors and subscription information:
http://www.tandfonline.com/loi/gmcl20

Plastic Deformation-Induced Orientation of Kaolinite Nanocrystals in Ultrahigh-Molecular Weight Polyethylene

V. V. Shapovalov [a], S. A. Schwarz [a], V. A. Shapovalov [b], E. E. Zubov [b], V. A. Beloshenko [b], S. F. Myronova [b], O. I. Aksimentyeva [c], M. H. Rafailovich [d] & V. I. Kozlov [e]

[a] Department of Physics, Queens College of the City, University of New York, Flushing, NY, USA

[b] Donetsk Physico-Technical Institute NASU, Donetsk, Ukraine

[c] Ivan Franko Lviv National University, Lviv, Ukraine

[d] Department of Materials Science and Engineering, Stony Brook, NY, USA

[e] Faculty of Physics, M. V. Lomonosov Moscow State University, Moscow, Russia

Version of record first published: 22 Sep 2010

Mol. Cryst. Liq. Cryst., Vol. 468, pp. 245/[597]–256/[608], 2007

ISSN: 1542-1406 print/1563-5287 online
DOI: 10.1080/15421400701230071

Plastic Deformation-Induced Orientation of Kaolinite Nanocrystals in Ultrahigh-Molecular Weight Polyethylene

V. V. Shapovalov
S. A. Schwarz
Department of Physics, Queens College of the City, University of New York, Flushing, NY, USA

V. A. Shapovalov
E. E. Zubov
V. A. Beloshenko
S. F. Myronova
Donetsk Physico-Technical Institute NASU, Donetsk, Ukraine

O. I. Aksimentyeva
Ivan Franko Lviv National University, Lviv, Ukraine

M. H. Rafailovich
Department of Materials Science and Engineering, Stony Brook, NY, USA

V. I. Kozlov
Faculty of Physics, M. V. Lomonosov Moscow State University, Moscow, Russia

The article deals with the investigation of the kaolinite plate orientation in ultra-high-molecular polyethylene. Kaolinite nanocrystals are in the form of thin plates, usually they are nanocrystalline materials. Samples of different degree of kaolinite plate ordering in ultra-high-molecular polyethylene were prepared by the solid phase extrusion. In the article, the degree of kaolinite ordering was investigated by two methods. The first method is based on studying the angular dependence of the EPR spectrum for Fe^{3+} ions which are present in natural kaolinite as an impurity. The second method is the X-ray diffraction technique. The both methods have shown that the solid-phase extrusion enables one to produce composites with kaolinite filler plates ordered in direction of the extrusion gradient.

Address correspondence to V. V. Shapovalov, Department of Physics, Queens College of the City, University of New York, Flushing, NY 11367, USA. E-mail: vshapovalov@hotmail.com; aksimen@org.lviv.net

Keywords: EPR spectrum; kaolinite nanocrystal; low temperature; polymeric composites

INTRODUCTION

Kaolin is widely used for producing filled polymeric systems [1–7]. Kaolin additions reduce the relative fraction of polymer in the final product, thus reducing cost and enabling one to create materials with a new complex of properties. Some of the properties depend on the relative orientation of kaolinite crystals. Kaolinite crystals are in the form of thin plates, usually they are nanocrystalline materials. However, the authors of paper [8] found a rather large kaolinite single crystal having dimensions of $0.2 \times 0.2 \times 0.01\,mm^3$. The problem of investigating the location of kaolinite crystals in polymer matrix is of current interest [4–6]. One prospective method of producing polymer materials with a preset orientation of filler crystals is solid-phase extrusion [7], where the orientational drawing is realized under high hydrostatic pressure. Articles [9–13] were the first to deal with the investigation of high-pressure effects on polymers. Principal regularities in the behaviour of polymer materials during deformation under high pressures are set forth in articles [14–18].

This article is aimed at studying the orientation of kaolinite crystal plates in ultrahigh-molecular weight polyethylene (UHMPE) induced by solid-phase extrusion by means of the X-ray diffraction and EPR spectroscopy methods.

To study the orientation of kaolinite nanosingle crystals by the EPR method, the ion of iron transition group Fe^{3+} was taken as a magnetic probe. The usage of $3d^n$ – ions of iron transition group in the capacity of magnetic probes is rather promising since they are very sensitive to physical states of their ligand and molecular environment and to magnetic and electrical fields. Such magnetic probes can feel value and symmetry of the crystalline field in structures with different symmetry order. In the investigated material, kaolinite nanocrystals arranged in the matrix of ultrahigh – molecular weight polyethylene differently. That's why the fine structure of EPR spectra of $3d^n$ – ions of iron transition group could not be used to investigate the magnetic anisotropy of the probe neither in the unit cell of the single crystal nor in macromolecule. In recent investigations [22–28] the magnetic probe Fe^{3+} has been found to be unique for investigating such magnetic anisotropy. The uniqueness is in the appearance of the anisotropic line with the g – factor equal to 4 in the EPR spectra of powder materials [22–28].

RESULTS

Method of Sample Preparation

Polymeric composite material based on UHMPE with 27% content of kaolin-clay is investigated in this article. The initial powder material was prepared by means of polymerization filling [19]. In this case, monomer polymerization occurs on the surface of filler (kaolinite). As a result, kaolinite single crystals are covered with a polymer layer of controllable thickness. The uniformity in polymer distribution on the kaolinite surface provides a uniform distribution of filler in the polymeric matrix.

The investigated samples were produced by the plunger extrusion method using a setup mounted on the basis of a 100 ton vertical hydraulic press. The setup included a deforming die located in the bottom of container bore. The plunger velocity was 2 mm/s. Billets for the extrusion were produced by compacting the powder in a mold.

Next, the billets were loaded in the high-pressure container. Prior to the extrusion, the container with the billet and die were heated to $T = 393\,K$, corresponding to $0.9T_m$, where T_m is the melting temperature of ultrahigh-molecular weight polyethylene. The temperature of extrusion was fitted empirically proceeding from the fact that quality specimens could not be produced at a lower or a higher temperature.

The extrusion ratio is the ratio between cross-section areas of the billet (container bore) and die opening found by the relation $\lambda = d_b^2/d_d^2$. Specimens with $\lambda = 7$ were investigated.

Kaolinite Structure

According to [8], the crystalline structure of kaolinite $Al_2[Si_2O_5] \cdot (OH)_4$ consists of two-layer packets with one tetrahedral silicon-oxygen layer of composition $[Si_{2n}O_{5n}]^{2n-}$ and one octahedral alumo-oxygen-hydroxylic layer of composition $[Al_{2n}(OH)_{4n}]^{2n+}$ (Fig. 1). Both layers form a packet by means of common oxygen atoms from the silicon-oxygen layer. The kaolinite space group is $C_i^1(P\bar{1})$. Unit cell parameters are: $a = 5.14$; $b = 8.93$; $c = 7.37$ E; $\alpha = 91.8^\circ$; $\beta = 104.5^\circ$.

In kaolinite, the paramagnetic impurity Fe^{3+} ions substitute the Al^{3+} ions isovalently. The iron content of kaolin varies usually from 0.3 to 1.1% depending on a deposit [20]. In Figure 1 it is seen that the existence of two nonequivalent positions of the magnetic Fe^{3+} ion are possible. In those positions the environment is represented by octahedra of two types with two oxygen atoms and four OH-groups.

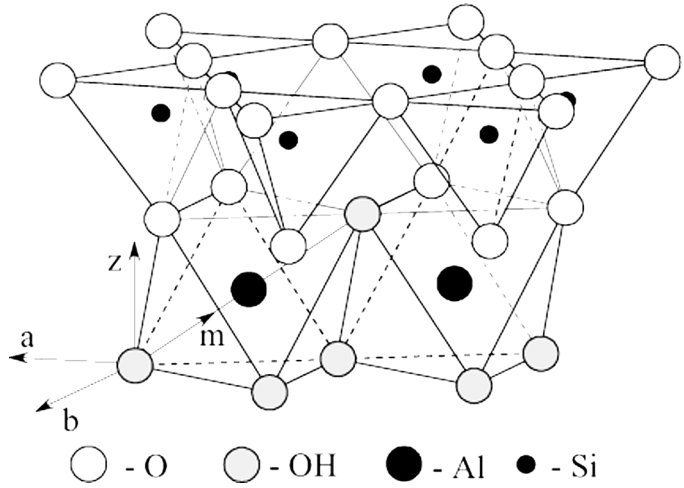

FIGURE 1 Structure of kaolinite $Al_2[Si_2O_5](OH)_4$: **a**, **b** – crystallographic axes; **m** – magnetic axis; Z – axis perpendicular to the (**ab**)-plane.

Experimental Results. X-ray Diffraction Analysis

The X-ray diffraction analysis of the kaolinite-plate orientation in extruded specimens was done at $T = 295$ K. A spectrograph was used to investigate the diffuse scattering of the low-intensity X-rays in a wide range of the X-ray scattering angles ($\theta = 5 \div 80^\circ$) with a high resolution of diffraction maxima provided by application of the Debye method and the use of a soft CrK_α-radiation, $\lambda = 2.29092$ E.

The X-ray diffraction pattern of Figure 2 corresponds to a powder sample with maximally disordered kaolinite plates. Figure 3 shows the X-ray results from the lateral surface of the extrudate and Figure 4 – from its face.

The X-ray diffraction patterns are characteristic of the presence of two regions differing in the values of intensities and the width of Debye lines. The first region lies in the interval of angles $\Delta\theta_1 = 9 \div 20^\circ$. Here the lines are more intense as compared to those of the second region. The second region is the interval of angles $\Delta\theta_2 = 20 \div 80^\circ$. For the X-ray diffraction patterns of Figures (2–4) the comparison of the intensities and widths of Debye lines in the two regions shows that:

1. In the case of the powder specimen, the Debye lines are wide. They are poorly-resolved for all diffraction angles. For the first region the maximum intensity of lines is $J_{max} = J_{0(1)} \approx 35$ a.u. That of the second region is $J_{max} = J_{0(2)} \approx 8$ a.u.

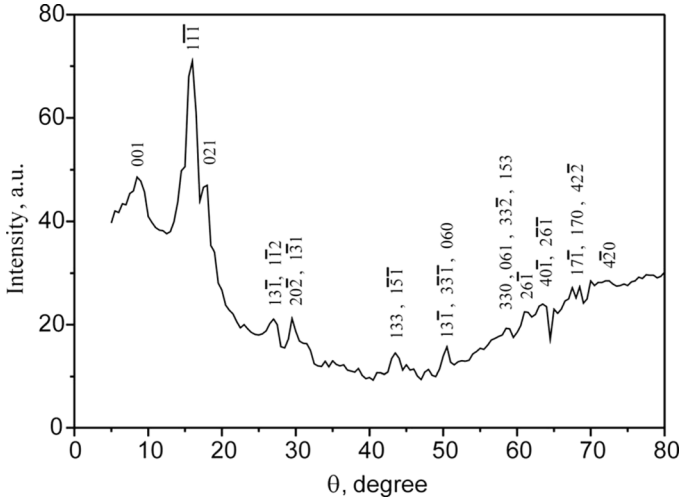

FIGURE 2 X-ray diffraction pattern of a powder sample.

2. The X-ray diffraction patterns from the first region correspond to the lateral surface of the extruded specimen, they are the most narrow and intense (Fig. 3), $J_{max} = J_{\|(1)} \approx 70$ a.u. In the second region $J_{max} = J_{\|(2)} \approx 6$ a.u. The width of the most intense lines of 001 and $1\bar{1}0$ from the corresponding basal planes reaches 0.45°.

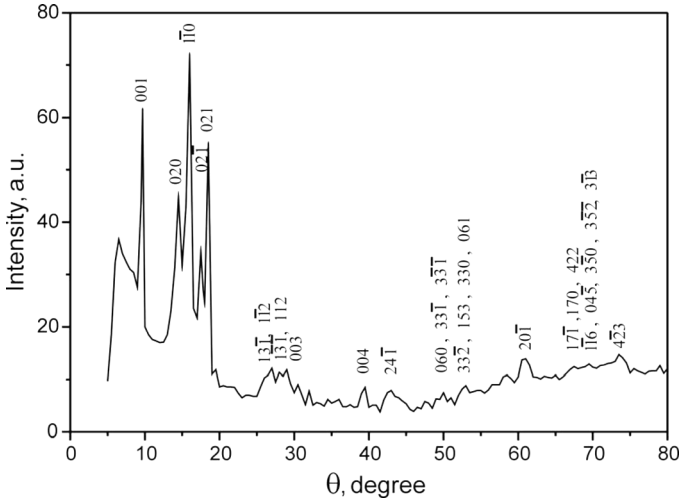

FIGURE 3 X-ray diffraction pattern of the lateral surface of the extruded sample. In the insert - a portion of the diffraction pattern at $\Delta\theta_1 = 9 \div 20°$.

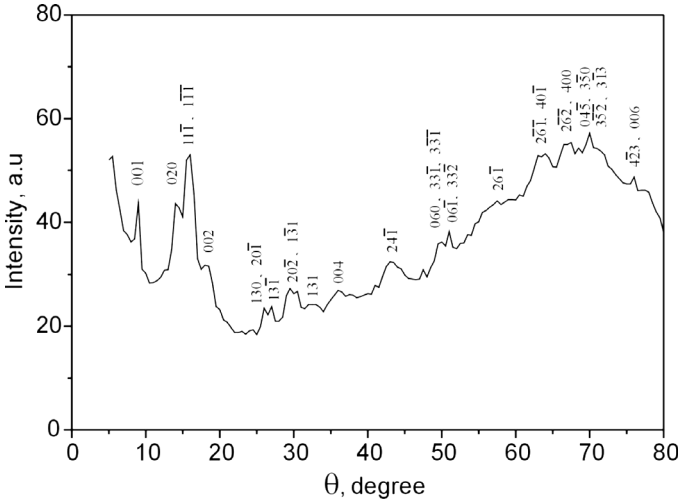

FIGURE 4 X-ray diffraction pattern of the face of extruded sample.

3. For the extrudate face (Fig. 4) the diffraction lines in the first region are less intense than those from the lateral surface (($J_{max} = J_{\perp(1)} \approx 35$ a.u.). In the second region the lines are more intense ($J_{max} = J_{\perp(2)} \approx 15$ a.u.).

It should be noted that in all the investigated cases the second regions differ. Near $\theta \approx 70^\circ$ the X-ray diffraction patterns for both the powder and the extrudate (Figs. 2,4) have a maximum which is the sum of diffraction lines of kaolinite plates with high indices hkl and diffuse incoherent scattering. Also, in the case of complete misorientation (powder), the value of this maximum is less than that of the extrudate (face) since the deformation-induced displacements of structure elements result in the increase in the intensity of incoherent large-angle θ scattering (background).

In the second region of angles, there is no such broad maximum for the lateral surface (Fig. 3). Thus, in the lateral surface layer the structure is more ordered than in the face layer. Also, the results indicate that in the lateral surface layer of the extrudate there has been a reorientation in the set of planes: $(1\bar{1}\bar{1}) \longrightarrow (1\bar{1}0)$.

One should pay attention to indices of lines from planes giving reflections in the region of small angles ($\theta < 20^\circ$), see Figure 3. In the case of diffraction from the initial powder, the maximum intensity is for the diagonal planes of the $(1\bar{1}\bar{1})$ type. For the basal planes of the (001) type the intensity is three times less (Fig. 2). A similar pattern

but with more narrow lines (Fig. 4) is observed for the extrudate face. On the diffraction pattern from the lateral surface layer of the extrudate, the $1\bar{1}\bar{1}$ line (the insert of Fig. 3) is very faint. At the same time, the most intense are reflections from the basal planes of (001) and $(1\bar{1}0)$ which are, respectively, parallel and normal to the (**ab**)-plane, Figure 1.

From the obtained results it can be concluded that:

1. The solid-phase extrusion of the composite material has resulted in the appearance of volume anisotropy in kaolinite. This is evidenced by differences in the intensities of Debye lines $J_{\parallel}$ from the lateral surface layer of the extruded specimen and $J_{\perp}$ from the face surface layer. In the first region of angles $J_{\parallel(1)}/J_{\perp(1)} = 2$. In the second region of angles $J_{\parallel(2)}/J_{\perp(2)} = 0.4$.
2. There is a preferable turn of kaolinite planes of low hkl indices along the cylinder axis. This is proved by a higher value of $J_{\parallel}/J_{\perp}$ ratio for the first region of angles as compared to that for the second region. For the first region $J_{\parallel(1)}/J_{0(1)} = 2$ and for the second one $J_{\parallel(2)}/J_{0(2)} = 0.75$.

After the extrusion the $(1\bar{1}0)$ and (001) planes of kaolinite plates take the preferential direction which is parallel to cylindrical specimen axis. This is evidenced by the maximum value of the intensities of lines from the $(1\bar{1}0)$ and (001) planes.

Experimental Results. Investigation of the EPR Spectrum

The EPR spectrum was investigated by using a spectrometer with the microwave field frequency $\nu = 9.247 \pm 0.001\,\text{GHz}$ at $T = 4.2\,\text{K}$. Primary attention was paid to the spectrum of the impurity Fe^{3+} ion, a component of kaolinite mineral.

The form of the EPR spectrum is shown in Figure 5. The spectrum of the impurity Fe^{3+} ion consists of two resonance lines. Line 1 at $T = 4.2\,\text{K}$ is anisotropic, it is described by the effective g-factor $g_1 = 4.13 \pm 0.16$. Resonance line 2 is described by the effective g-factor $g_2 = 2.15 \pm 0.1$. At $T = 4.2\,\text{K}$ it has the width $\Delta H_{2pp} = 0.36\,\text{kOe}$.

In the EPR spectrum there are, apart from the resonance lines pertaining to the impurity Fe^{3+} ion, more narrow ($\Delta H \approx 17$ Oe) resonance lines of the Cr^{3+} ion and O_2^- ion. The Cr^{3+} EPR spectrum was used for magnetic field calibration. (Cr^{3+}- ions are not kaolinite components). According to [20], O_2^- ions are located on cleavage planes of the mineral. The O_2^- EPR spectrum is in the form of a narrow line described by a g-factor equal to two.

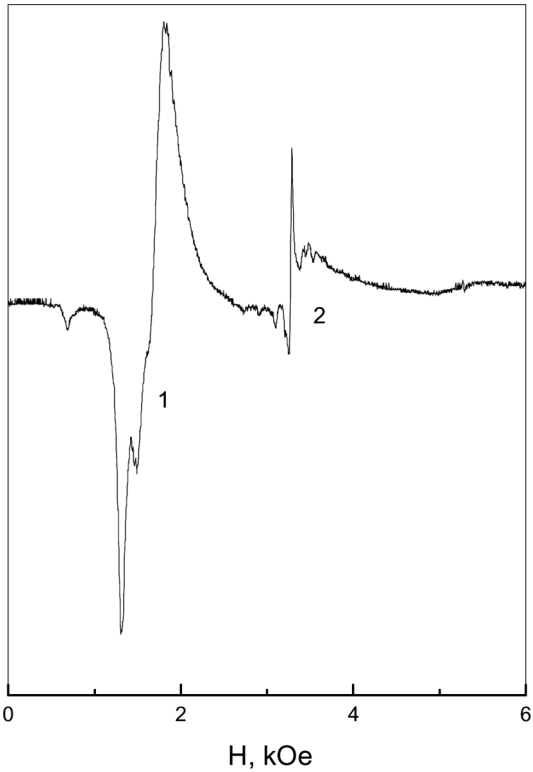

FIGURE 5 Fe^{3+} EPR spectrum in kaolinite: T = 4.2 K, H//Z.

Dependence of the EPR spectrum on magnetic-field orientation has been investigated in two planes, normal to the extrudate axis and parallel to the same. In the first case, the dependence of the EPR spectrum on magnetic field orientation was not found. In the second case, the dependence is that of the resonance field of line 1 on the angle of rotation (Fig. 6).

The angular dependence of Figure 6 contains the two groups of conjugate maxima. The maxima A1 and A2 shifted by 180° relative to each other pertain to the first group. The maxima B1 and B2, which are also 180°-shifted pertain to the second group. Those conjugate maxima of the angular dependence of the resonance field define the directions along which the axes of Fe^{3+} magnetic centers are preferentially oriented.

It should be noted that the axes of symmetry of the magnetic centers corresponding to the maxima (A1, A2) and (B1, B2) are turned

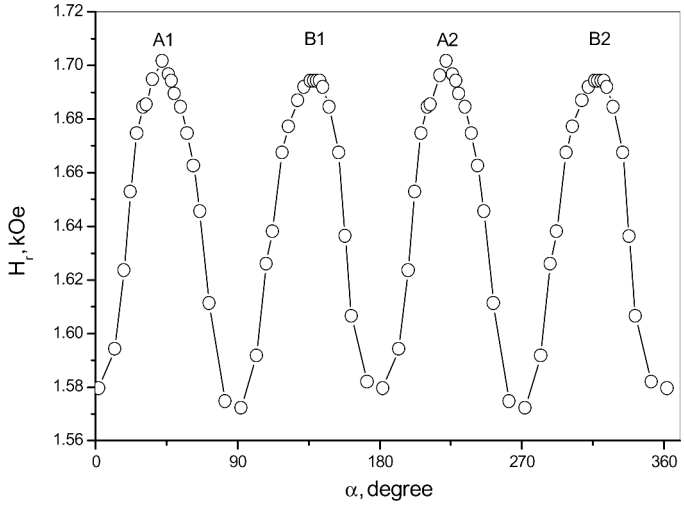

FIGURE 6 Angular dependence of the resonance field of line 1 at $T = 4.2\,K$ in the plane parallel to the cylinder axis.

by angles other than 90°. Angles between the axes are 96° and 84°. This is because of peculiarities in orientation of kaolinite plates in the extruded specimen. The observed angular dependence of Fe^{3+} EPR spectrum shown in Figure 6 needs additional discussion, and this is done in Section 6.

DISCUSSION

The Fe^{3+} ion has a configuration $3d^5$. The spin of the ground state is $S = 5/2$. The most frequently encountered Fe^{3+} EPR spectra have typical g-factor values close to $g \cong 2$.

The observed EPR spectrum has, on the one hand, features typical of a powder or an amorphous substance. On the other hand, the angular dependence indicates that in the extruded specimen the axes of symmetry of the magnetic centers are to a considerable degree oriented along specific directions. From this viewpoint, the obtained EPR spectrum should be considered as partially averaged with respect to directions of the magnetic center axes of symmetry.

In article [21] a detailed review is given of EPR spectral investigations for iron ions in substances with the misoriented directions of the axes of symmetry of magnetic centers. It is assumed that the spectrum consisting of two resonance lines with $g \cong 2$ and $g \cong 4.3$ pertains to different nonequivalent magnetic centers of Fe^{3+} ion. The difference is

in values of the low-symmetry component of the crystal field affecting the magnetic ion. The authors [21] of the above-mentioned article believe that the line with $g \cong 2$ corresponds to the center with the low-symmetry component of the crystal field much less than the Zeeman energy. The line with $g \cong 4.3$ corresponds to the center with the low-symmetry component of the crystal field much larger than the Zeeman energy.

In kaolinite there are two nonequivalent positions of the magnetic ion (Fig. 1). On the other hand, in mineral kaolin the magnetic centers may be accidentally deformed. In the totality of magnetic centers, one part may be deformed weakly, so that for those centers, the parameter of the zero splitting D will be smaller than the microwave field quantum ($D < h\nu$). Such magnetic centers will contribute to the resonance line 2. The rest of the magnetic centers contribute to the formation of line 1. Apart from the above mechanisms of formation of the two resonance lines in the Fe^{3+} EPR spectrum, a third mechanism should be recognized. It is defined by peculiarities of dynamic deformations of the magnetic-ion crystalline environment. The mechanism is described in article [22] in more detail.

The spin Hamiltonian of the magnetic ion is represented as

$$H_0 = g_0 \cdot \beta \cdot \boldsymbol{H} \cdot \boldsymbol{S} + D \cdot (S_z^2 - S(S+1)/3) + E \cdot (S_x^2 - S_y^2) \qquad (1)$$

where β – is the Bohr magneton, g_0 is the g-factor of the ground multiplet $S = 5/2$. The value of g_0 is close to 2.0; S_x, S_y, S_z – are spin-operator components; D, E are parameters of the zero splitting. D characterizes the field of axial symmetry. E characterizes the rhombic component of the field.

The value of the effective g-factor and the angular dependence of the EPR spectrum of the resonance line 1 of Fe^{3+} magnetic centers are described in article [21]. According to [21], the effective g-factor of the resonance line 1 is described by the relationship

$$g = \frac{30}{7}\left\{1 + \frac{4}{7}q(\ell_z^2 - \ell_y^2) + \frac{4}{49}(15q^2 + 4p^2)(\ell_y^2 + \ell_z^2) - \frac{2}{49}(4q^2 + 5p^2)(\ell_y^2 - \ell_z^2) - \frac{24}{343}(17q^2 + 4p^2)\right\} \qquad (2)$$

where $q = (D - 3E)/(D + E)$, $p = (g\mu_B H)/(D + E)$, $\ell_x = \sin\theta \cdot \cos\varphi$, $\ell_y = \sin\theta \cdot \sin\varphi$, $\ell_z = \cos\theta$. Angles θ, φ assign the direction of the external magnetic field in the spherical system of coordinates.

For the octahedral environment, the principal axis of symmetry of the magnetic center, as a rule, coincides with one of the fourth-order axes of the ligand octahedron. In Figure 1, this magnetic axis is denoted by vector **m**. For the regular octahedron this angle is at 57°

with respect to axis Z normal to the (**ab**)-plane, which coincides with the most developed cut plane of the kaolinite crystal. In the case of rhombic or a lower symmetry of the magnetic center, the magnetic axis of symmetry can deviate from the axis of the distorted ligand octahedron by an angle larger than 10°. Angle $\alpha = 0^\circ$ of Figure 6 corresponds to a direction of the external magnetic field along the axis of the extruded sample. According to the angular dependence of Figure 6, the magnetic axis is directed at an angle of 48° to axis Z (Fig. 1). From the analysis of the experimental angular dependence shown in Figure 6 and of the dependence for the effective g-factor (2) it can be concluded that the Z-axis of each kaolinite plate is preferentially oriented normal to extrudate axis. That is, the (**ab**)-planes of kaolinite plates are preferentially oriented along the axis of the extruded specimen.

By the X-ray diffraction investigations, it was found that the (**ab**)-planes of kaolinite plates take a preferential direction which is parallel to the axis of the specimen. That is, the Z-axis turns out to be located along the face layer of the specimen, thus fitting the EPR data.

CONCLUSIONS

The obtained results make it possible to conclude that the solidphase extrusion orders the kaolinite plates in ultra-high-molecular polyethylene. The character of their orientation is determined by direction of the deformation gradient and its value. Such preferential orientation of kaolinite plates is seen on the angular dependence of the resonance field of the EPR spectrum for Fe^{3+} ions which are contained in kaolinite single crystals as an impurity. The angular dependence maxima determine the marked directions along which the axes of magnetic centers of the Fe^{3+} ions are preferentially oriented. A preferential turn along the direction of extrusion is for kaolinite planes having low hkl indices. This is indicated by the maximum value of the $(1\bar{1}0)$ and (001) plane intensities.

REFERENCES

[1] Vasyukov, V. N., Shapovalov, V. V., Schwarz, S. A. *et al.* (2002). *J. Magn. Res.*, *154*, 15.
[2] Hu, X., Zhang, W., Rafailovich, M. *et al.* (2001). *Mat. Res. Soc. Proceedings Series*, NY, USA.
[3] Vaia, R. A. & Giannelis, E. P. (2001). *MRS Bulletin*, May 2001, USA, 394–401.
[4] Howard, E. G., Lipscomb, R. D., MacDonald, R. N. *et al.* (1981). *Synthesis, Ind. Eng. Chem. Product. Research and Development*, *20*, 421.

[5] Lim, Y. T. & Ok Park, O. (2000). *Macromol. Rapid Commun.*, *21*, 231.
[6] Alexandre, M. & Dubois, P. (2000). *Materials Science and Engineering*, *28*, 1.
[7] Beloshenko, V. A., Kozlov, G. V., & Varyuhin, V. N., Slobodina, V. G. (1997). *Acta Polymer*, *48*, 181.
[8] Druts, V. A. & Kashaev, A. A. (1960). *Kristallographiya*, *5*, 224.
[9] Dow, R. B. (1939). *J. Chem. Phys.*, *7*, 201.
[10] Parks, W. & Richards, R. B. (1949). *Trans. Faradey Soc.*, *45*, 203–211.
[11] Weir, C. E. (1951). *J. Res. Natl. Bur. Stand.*, *46*, 207.
[12] Weir, C. E. (1953). *J. Res. Natl. Bur. Stand.*, *50*, 95.
[13] Bridgman, P. W. (1953). *J. Appl. Phys.*, *24*, 560.
[14] Pae, K. D. & Bhateja, S. K. (1975). *J. Macromol. Sci. C*, *13*, 1.
[15] Bhateja, S. K. & Pae, K. D. (1975). *J. Macromol. Sci. C*, *13*, 77.
[16] Kishore, K. & Vasanthakumari, R. (1984). *High Temp.–High Pres.*, *16*, 241.
[17] Prut, E. V. (1994). In: *High – pressure Chemistry and Physics of Polymers*, Kovarskii, A. L. (Ed.), CRC Press: Bosa Raton, 341.
[18] *Ultra – high modulus polymers*/Edited by A. Ciferri and I. M. Ward., London, 271 (1979).
[19] Adelman, R. L. & Howard, E. G. *Pat.* 41511226, USA.
[20] Mank, V. V., Ovcharenko, F. D., Golovko, L. V. *et al.* (1975). *DAN SSSR*, *223*, 389.
[21] Klyava, Ya. G. (1988). *EPR Spectroscopy of Disordered Solids*, "Zinatne", Riga, P.P. 320.
[22] Vasyukov, V. N., Dyakonov, V. P., Shapovalov, V. A., Aksimentyeva, E. I., Szymczak, H., & Piechota, S. (2000). *Low Temperature Physics*, *26*, 265–269.
[23] Aksimentjeva, E. I., Dyakonov, V. P., Shapovalov, V. V. *et al.* (2000). *Zhurnal Obshej Khimii*, *70*, 1680.
[24] Vasyukov, V. N., Shapovalov, V. V., Schwarz, S. A. *et al.* (2002). *J. Magn. Resonance*, *154*, 15.
[25] Vasyukov, V. N., Shapovalov, V. A., Dyakonov, V. P. *et al.* (2002). *Int. J. Quantum Chemistry*, *88*, 425.
[26] Vasyukov, V. N., Shapovalov, V. V., Shapovalov, V. A. *et al.* (2002). *Mol. Cryst. Liq. Cryst.*, *384*, 13.
[27] Shapovalov, V. V., Schwarz, S. A., Shapovalov, V. A. *et al.* (2004). *Abstracts of 6-th Int. Conf. EXCON'04*, July 6–9, 2004, Cracow: Poland, 25.
[28] Shapovalov, V. V., Schwarz, S. A., & Shapovalov, V. A. (2005). *Mol. Cryst. Liq. Cryst.*, *426*, 21.